

Scaling of laser produced plasma UTA emission down to 3 nm for next generation lithography and short wavelength imaging

Bowen Li^a, Akira Endo^b, Colm O’Gorman^a, Takamitsu Otsuka^c, Thomas Cummins^a,
Tony Donnelly^a, Deirdre Kilbane^a, Padraig Dunne^a, Gerry O’Sullivan^a, Weihua Jiang^d,
Takeshi Higashiguchi^{*c,e,f}, and Noboru Yugami^{c,e,f}

^aSchool of Physics, University College Dublin, Belfield, Dublin, Ireland 4;

^bResearch Institute of Science and Engineering, Waseda University, 3-4-1, Okubo, Shinjuku-ku,
Tokyo, Japan 169-0072;

^cDepartment of Advanced Interdisciplinary Sciences, Utsunomiya University,
Yoto 7-1-2, Utsunomiya, Tochigi, Japan 321-8585;

^dDepartment of Electrical Engineering, Nagaoka University of Technology, Kami-tomiokamachi
1603-1, Nagaoka, Niigata, Japan 940-2188;

^eCenter for Optical Research & Education (CORE), Utsunomiya University,
Yoto 7-1-2, Utsunomiya, Tochigi, Japan 321-8585;

^fJapan Science and Technology Agency, CREST,
4-1-8 Honcho, Kanagawa, Saitama, Japan 332-0012

ABSTRACT

An engineering prototype high average power 13.5-nm source has been shipped to semiconductor facilities to permit the commencement of high volume production at a 100 W power level in 2011. In this source, UTA (unresolved transition array) emission of highly ionized Sn is optimized for high conversion efficiency and full recovery of the injected fuel is realized through ion deflection in a magnetic field. By use of a low-density target, satellite emission is suppressed and full ionization attained with short pulse CO₂ laser irradiation. The UTA is scalable to shorter wavelengths, and Gd is shown to have similar conversion efficiency to Sn (13.5 nm) at a higher plasma temperature, with a narrow spectrum centered at 6.7 nm, where a 70% reflectivity mirror is anticipated. Optimization of short pulse CO₂ laser irradiation is studied, and further extension of the same method is discussed, to realize 100 W average power down to a wavelength of 3 nm.

Keywords: Extreme ultraviolet, water window, unresolved transition array (UTA), rare-earth, LPP

1. INTRODUCTION

In recent years, laser-produced dense plasmas have been focused on as high efficiency and high power sources of extreme ultraviolet (EUV) radiation. The development of sources of EUV emission with a wavelength less than 10 nm is a subject of considerable interest. Wavelengths shorter than 10 nm are especially useful for next generation semiconductor lithography toward the final stage beyond the 13.5-nm EUV source [1] and for other applications, such as material science and biological imaging near the water window. In particular, in our setup, EUV emission at the relevant wavelength is coupled with a Mo/B₄C and/or La/B₄C multilayer mirror with a reflective coefficient of 40% at 6.5–6.7 nm [2].

* Further author information: (Send correspondence to T.H)

Present address (T.H): E-mail: higashi@cc.utsunomiya-u.ac.jp, +81 28 689 6087

Before characterizing the high power rare-earth element plasma EUV source for 6.5–6.7 nm, it is important to summarize the properties of efficient EUV sources at 13.5 nm. Many research groups for semiconductor lithography have reported efficient EUV source schemes, which are attributed to $n = 4 - n = 4$ transitions in tin (Sn) ions that overlap to yield an intense unresolved transition array (UTA) [3], coupled with a Mo/Si multilayer mirror. To increase the conversion efficiency (CE) in laser-produced Sn plasmas, it is important to reduce both the self-absorption in the plasmas [4] and the plasma hydrodynamic expansion loss effect [5] at an electron temperature of 20–30 eV. A maximum CE of 3–4% has been predicted for Nd:YAG lasers irradiating at a laser intensity of 10^{11} W/cm² with pulse durations of a few ns, while for CO₂ lasers, because of reduced opacities, a higher CE should be obtained at a laser intensity of 10^{10} W/cm² [6–8]. The rare-earth elements of gadolinium (Gd) and terbium (Tb), on the other hand, produce strong narrow band emission, which again is attributed to a $n = 4 - n = 4$ UTA, at 6.7 nm. The spectral behavior of Gd and Tb plasmas is expected to be similar to that of Sn plasmas, because of the similar atomic structure of 4*d* open-shell ions [9]. Previous work on rare-earth plasma EUV sources, however, has been focused on absorption spectroscopy by generating quasicontinuum spectra at low laser power [10,11]. Recently, the UTA emitted from these plasmas have been investigated for high power sources [12]. However, no fundamental research has been reported for the 6.7-nm focused spectral behavior and its dependence on various parameters. EUV emission around 6.5–6.7 nm should be tuned for use with the Mo/B₄C and/or the La/B₄C multilayer mirrors to realize powerful practical sources.

Recently, the suitability of Nd:YAG (Nd:yttrium-aluminum-garnet) laser-produced plasma EUV sources based on Gd and Tb has been demonstrated for high power sources [13]. According to our previous study [13], self-absorption effects in Gd and Tb plasmas are significant, as evidenced by their laser wavelength dependence and the results of dual laser pulse irradiation experiments. Consequently, the emitted spectra and CE are a trade-off between EUV line emission and self-absorption as the plasmas are optically thick at 6–7 nm. The spectra of these resonance lines around 6.7 nm suggest that the in-band emission increases with increased plasma volume by suppressing the plasma hydrodynamic expansion. In addition, to increase the conversion efficiency (CE) and the spectral purity, we have proposed the use of shorter pulse duration irradiation, a low initial density target and low electron density plasmas (such as CO₂ laser-produced plasmas and/or discharge-produced plasmas) [13]. Apart from one previous study [11], no systematic investigation has been reported on the sensitivity of the 6.7-nm spectral behavior and conversion efficiency to various parameters, such as laser wavelength and initial target density. In order to assess the suitability of Gd plasmas as efficient EUV sources, their detailed emission properties, including self-absorption effects, need to be clarified. From the perspective of semiconductor lithography, optimization of the laser irradiation conditions and target composition are needed to guide source development to realize powerful practical sources with high EUV conversion efficiency (CE) from laser energy to EUV emission energy. It is important to study plasmas produced by solid-state lasers operating at a typical wavelength of 1 μ m as, in future, high power and high repetition rate operation fiber lasers will be used to produce high temperature plasmas [14].

In this paper, we report the UTA spectral scaling to shorter wavelengths, and Gd is shown to have similar conversion efficiency to Sn (13.5 nm) at a higher plasma temperature, with a narrow spectrum centered at 6.7 nm, where a 70% reflectivity mirror is anticipated. Optimization of short pulse CO₂ laser irradiation is studied, and further extension of the same method is discussed, to realize 100 W average power down to a wavelength of 3 nm.

2. MULTI CHARGED-STATE IONS OF GADOLINIUM AT 6.X NM

Figure 1(a) shows the ion population of the Gd as a function of the electron temperature in the steady-state collisional-radiative (CR) model at an electron density of 1×10^{21} cm⁻³ [15]. The dominant species originate at an electron temperature of 30–150 eV. A range of ion stages is present in a plasma at any given electron temperature, where higher temperatures produce higher ion stages. For example, in a Gd plasma, the 4*d*–4*f* and 4*p*–4*d* transitions in ions from Gd¹²⁺ and Gd²⁵⁺ form a UTA around 6.5–6.7 nm at electron temperatures of 50 and 120 eV, respectively. Theoretical weighted oscillator strength *gf* spectra calculated with the FAC code are presented in Figs. 1(b) and 1(c) to show the resonant emission [16] in ions ranging from Gd¹²⁺ to Gd²⁵⁺, which produces the strong band emission.

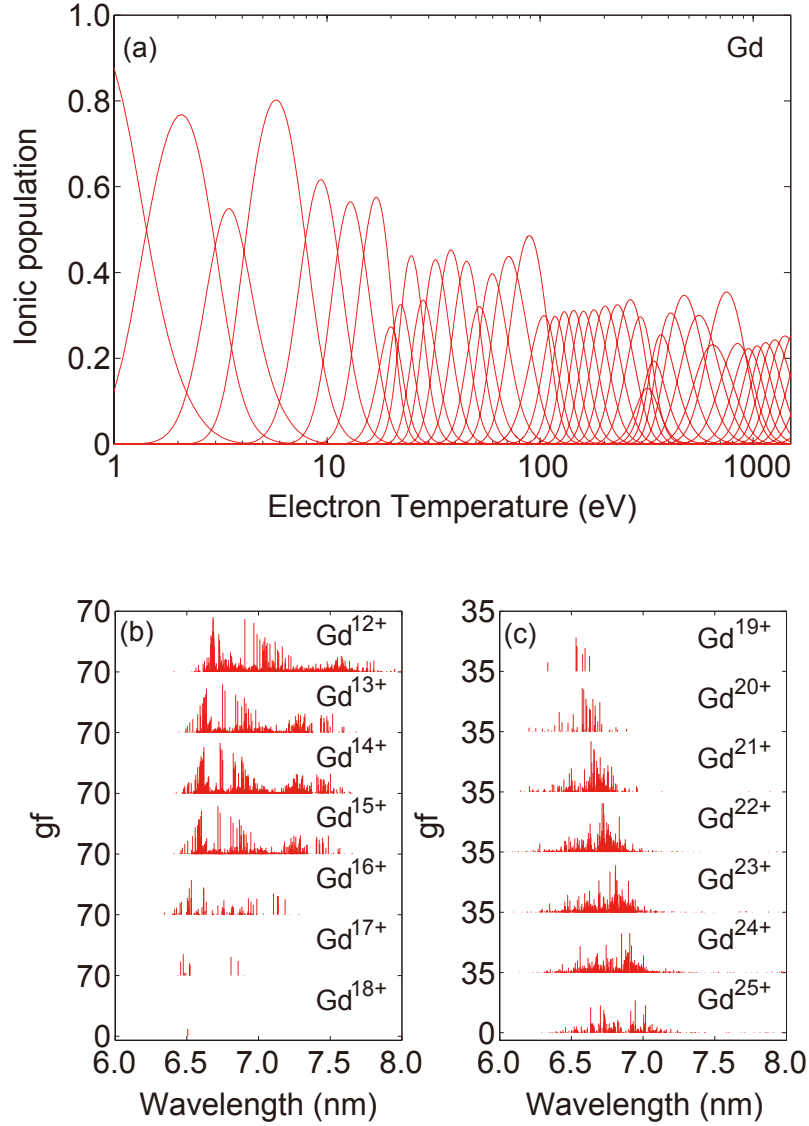


Fig. 1. Electron temperature dependence of the Gd (a) ion population according to the steady-state CR model. The weighted oscillator strength spectra of the resonant lines for each contributing ion stage are shown in (b) and (c).

3. PROPERTY OF EUV EMISSION AT 6.X NM FROM RARE-EARTH GD PLASMAS

In this section, we report and discuss the EUV spectra and CE in the 6.5–6.7 nm region from Gd plasmas produced by the fundamental and the 2nd and 3rd harmonics of a Nd:YAG laser. To understand the effects of self-absorption, we observed the spectral behavior and the EUV CE and explored not only the influence of laser wavelength, which is reflected in differing electron (and ion) densities, but also the impact of Gd concentration in the target. As a result, we obtained an optimum conversion efficiency of 1.3% in this work [17,18].

A Q-switched Nd:YAG laser operating at 1064, 532, and 355 nm with pulse durations of 10, 8, and 7 ns (full width at half-maximum (FWHM)) was used. The laser was perpendicularly focused on planar Gd targets with a thickness of 1 mm with a 15-cm focal length lens. The focused intensity was varied from 10^{10} to 10^{12} W/cm² at a

focal spot size of 50 μm to compare the effects of laser wavelength. The laser was operated in a single shot mode. The absolute EUV energy, which was positioned at 45° with respect to the incident laser axis, was measured by use of a calibrated EUV energy meter equipped with a calibrated Mo/B₄C multilayer mirror [2] and a Zr filter. All EUV CE's presented here were evaluated based on the emission energy at 6.7 nm within a 2% bandwidth (BW) and for a solid angle of 2π sr, over which the radiation was assumed to be isotropic. A flat-field grazing incidence spectrometer with 1200 grooves/mm variable line space grating was positioned at 45° with respect to the incident laser axis. The time-integrated spectra were obtained with a thermoelectrically cooled back-illuminated x-ray CCD (charge coupled device) camera. The typical spectral resolution was better than 0.02 nm.

In order to observe the effects of differing critical electron densities, n_{ec} , on the plasma opacity ($n_{ec} \propto \lambda^2$, where λ is the laser wavelength), we observed the EUV spectra at the same laser intensity of approximately $1.6 \times 10^{12} \text{ W/cm}^2$ (laser energy: 320 mJ per pulse and spot diameter: 50 μm (FWHM)), as shown in Fig. 2. This laser intensity is not optimum and is used merely to compare the effects of differing laser wavelengths. The critical densities are $n_{ec} = 1 \times 10^{21}$, 4×10^{21} , and $9 \times 10^{21} \text{ cm}^{-3}$ at laser wavelengths of $\lambda = 1064$, 532, and 355 nm. The in-band emission at 6.7 nm, which is attributed to resonance lines, increased with increasing laser wavelength, resulting in the maximum emission for $\lambda = 1064$ nm. The corresponding EUV CE's were observed to be 1.1%, 0.7%, and 0.5% for laser wavelengths of $\lambda = 1064$, 532, and 355 nm. The intensity ratio between the resonant lines around 6.7 nm and the satellite emission at wavelengths longer than 7 nm decreased for the 532-nm and 355-nm laser pulses compared to the 1064-nm pulse. Even allowing for the presence of an underlying recombination continuum, from Fig. 2 it is seen that satellite emission at wavelengths longer than 7 nm increases with decreasing wavelength. The decrease of the 6.7-nm emission is attributed to self-absorption in the denser, short-wavelength plasma [19]. This behavior is supported by the results of a dual laser irradiation experiment to control the electron density gradient, i.e., the absorption length [20,21] which found that the emission intensity of Gd plasmas at 6.7 nm was almost constant [13]. The Gd spectrum therefore contains resonant UTA lines around 6.7 nm and many satellite emission lines at wavelengths longer than 6.7 nm if the density is sufficiently high. This spectral behavior is similar to that already reported for Nd:YAG laser-produced xenon (Xe) plasmas, which emit resonant lines around 11 nm and satellite lines at wavelengths longer than 11 nm, especially around 13.5 nm [22,23].

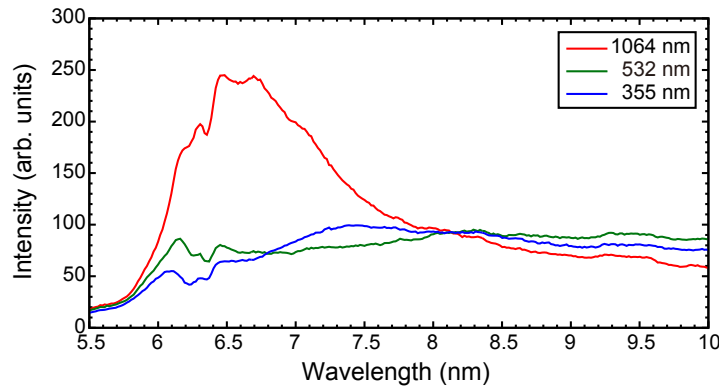


Fig. 2. EUV spectra at laser wavelengths of 1064 (red), 532 (green), and 355 nm (blue) for the same laser intensity of $1.6 \times 10^{12} \text{ W/cm}^2$ (laser energy: 320 mJ per pulse and spot diameter: 50 μm (FWHM)), respectively.

Figure 3(a) shows the dependence of the EUV CE on laser intensity at $\lambda = 1064$ nm, chosen in order to maximize the EUV emission as suggested by Fig. 3. The EUV CE increases with increasing laser intensity and the EUV CE was maximized at 1.1% at a laser density of $I_L \approx (1-1.5) \times 10^{12} \text{ W/cm}^2$ when a solid Gd target was used. The electron temperature is evaluated to be of the order of 120 eV or greater, at this laser intensity, by comparison with oxygen ion emission under identical experimental conditions.

To reduce the effects of self-absorption, it is important to study the influence of the initial concentration of Gd in the target. In order to increase of the spectral purity and the EUV CE, we used a low-density Gd target, similar to the low-density Sn targets used to optimize emission from 13.5-nm EUV sources [21,24,25]. The laser intensity

dependence of the EUV CE in Fig. 3(a) and the spectral purity in Fig. 3(b) are shown for $\lambda = 1064$ nm and a focused laser spot diameter of 50 μm for both solid Gd and low-density Gd_2O_3 . Again for the Gd_2O_3 target the EUV CE increased with the incident laser intensity and reached a maximum value of 1.3% at a laser intensity of approximately $1.5 \times 10^{12} \text{ W/cm}^2$. For solid Gd, the EUV CE also essentially saturates at laser intensities above $0.7 \times 10^{12} \text{ W/cm}^2$, which can be attributed to the wide electron temperature range over which ions with open $4d$ subshells dominate the plasma [13]. In the case of the lower-density Gd_2O_3 target, the EUV CE was observed to be 0.2% higher than for the solid target due to the reduction of self-absorption. This value could probably be further improved if the Gd concentration were further reduced. The spectral purity, defined as the ratio of intensity within the 2% bandwidth around 6.7 nm to that in the spectral range from 5.5 to 10 nm, increased with laser intensity and, in the case of the solid target, reached a maximum value of approximately 6%. For the Gd_2O_3 target, on the other hand, the spectral purity was almost constant at about 7% over the intensity range examined and was therefore marginally higher than that of the solid target.

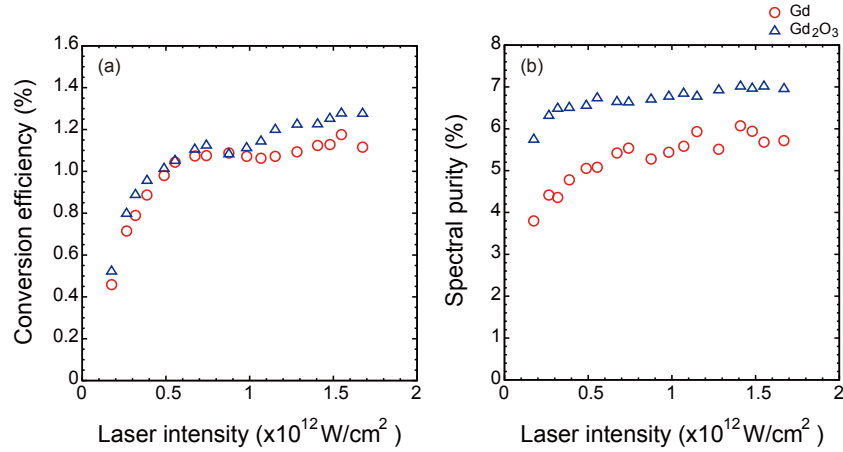


Fig. 3. Laser intensity dependence of the EUV CE (a) and spectral purity (b) on laser intensity at a laser wavelength of 1064 nm for a target containing 40% Gd (blue, rectangles) or 100% Gd (red, circles).

Figure 4 compares the spectra from the low-density and solid-density targets at a laser intensity of $1.6 \times 10^{12} \text{ W/cm}^2$. The resonant line emission is relatively higher due to the reduction of self-absorption. It is seen that the emission intensity increased for the low-density target, resulting in the achievement of a higher EUV CE of 1.3%. To increase the CE and the spectral purity these data suggest that it is important to use shorter pulse duration irradiation and low electron density plasmas (such as CO_2 laser-produced plasmas or discharge-produced plasmas) [13]. In

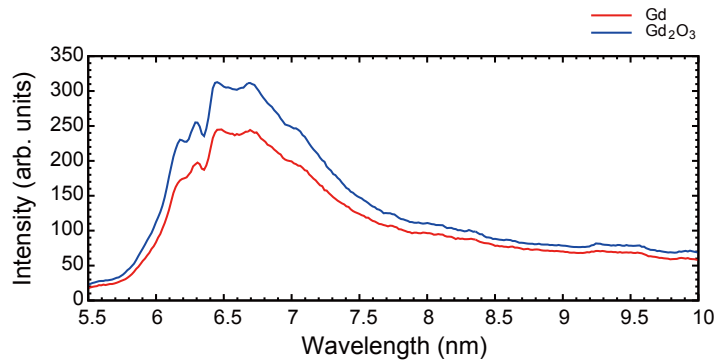


Fig. 4. Spectral comparison for the low- (blue) and the solid-density target (red) at different laser intensities of $1.6 \times 10^{12} \text{ W/cm}^2$.

addition, higher EUV CE would be expected if the laser source size were increased to reduce the plasma expansion loss [13].

4. UTA SCALING WITH ATOMIC NUMBER AND BI PLASMA EUV

Because it moves to shorter wavelength with increasing Z , the $n = 4 - n = 4$ UTA can be used for other applications, such as transmission x-ray microscopy for biological imaging in the water window (Fig. 5). This figure shows the calculated positions of the strongest $n = 4 - n = 4$ transitions for four stages of each element corresponding to Ru-like (red), Rh-like (blue), Pd-like (green) and Ag-like (black) ions. From this plot it is clear that maximum overlap between emission from different stages occurs in the lanthanides and corresponds from an atomic physics viewpoint to the localization of the 4f wavefunction in the ionic core where its overlap with the 4d changes little with ion stage [26]. For lower Z elements the emission extends over a broader energy range due to differing degrees of 4f localization while the 4p spin orbit splitting causes the emission to diverge to form two emission regions at the higher Z end.

Based on this result, we have made preliminary studies of the potential of Bi as a BEUV source. Our calculations show that Bi plasmas, at an electron temperature in the range 570 to 600 eV, radiate strongly near 3.9 nm. We have initiated a number of experiments to explore how this emission may be optimized in practice.

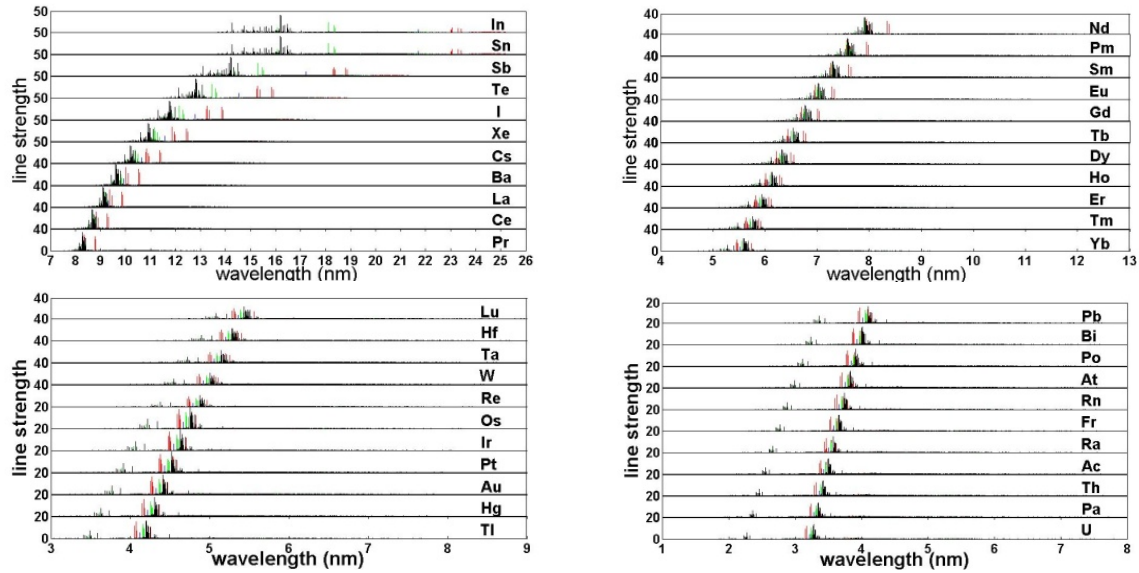


Fig. 5. Calculated position of $n = 4 - n = 4$ transitions in key ions in elements from indium ($Z = 49$) to uranium ($Z = 92$). The localization of emission near 6.7 nm in Gd and 3.9 nm in Bi is clearly evident.

6. SUMMARY AND OUTLOOK

In summary, we have observed the spectral behavior and measured the EUV CE around 6.7 nm for shorter wavelength EUV emission. As the effects of self-absorption on the strongest resonance lines in the Gd UTA are large, it is important to produce a low-density plasma. The highest conversion efficiency in this spectral region was observed to be 1.3%. To increase the CE and the spectral purity, it is important to produce low-density plasmas such as CO_2 laser-produced plasmas.

ACKNOWLEDGMENTS

The author acknowledges many collaborators, in particular W. Jiang and D. Kilbane. A part of this work was performed under the auspices of MEXT (Ministry of Education, Culture, Science and Technology, Japan) and “Utsunomiya University Distinguished Research Projects.” The UCD group acknowledges support from Science Foundation Ireland under Principal Investigator Research Grant No. 07/IN.1/B1771.

REFERENCES

- [1] D. T. Attwood, “*Soft X-Rays and Extreme Ultraviolet Radiation*” (Cambridge University Press, Cambridge, 2000), Chap. 6.
- [2] Fraunhofer IOF Annual Report 2007.
- [3] V. Bakshi, “*EUV Sources for Lithography*” (SPIE, Washington, 2006), Chap. 11.
- [4] S. Fujioka, H. Nishimura, K. Nishihara, A. Sasaki, A. Sunahara, T. Okuno, N. Ueda, T. Ando, Y. Tao, Y. Shimada, K. Hashimoto, M. Yamaura, K. Shigemori, M. Nakai, K. Nagai, T. Norimatsu, T. Nishikawa, N. Miyanaga, Y. Izawa, and K. Mima, “Opacity Effect on Extreme Ultraviolet Radiation from Laser-Produced Tin Plasmas,” *Phys. Rev. Lett.* **95**, 235004-1-235004-4, 2005.
- [5] R. C. Spitzer, T. J. Orzechowski, D. W. Phillion, R. L. Kauffman, and C. Cerjan, “Conversion efficiencies from laser-produced plasmas in the extreme ultraviolet regime,” *J. Appl. Phys.* **79**, pp. 2251-2258, 1996.
- [6] H. Tanaka, A. Matsumoto, K. Akinaga, A. Takahashi, and T. Okada, “Comparative study on emission characteristics of extreme ultraviolet radiation from CO₂ and Nd:YAG laser-produced tin plasmas,” *Appl. Phys. Lett.* **87**, 041503-1-041503-3, 2005.
- [7] Y. Ueno, G. Soumagne, A. Sumitani, A. Endo, and T. Higashiguchi, “Enhancement of extreme ultraviolet emission from a CO₂ laser-produced Sn plasma using a cavity target,” *Appl. Phys. Lett.* **91**, 231501-1-231501-3, 2006.
- [8] Y. Tao, M. S. Tillack, K. L. Sequoia, R. A. Burdt, S. Yuspeh, and F. Najmabadi, “Efficient 13.5 nm extreme ultraviolet emission from Sn plasma irradiated by a long CO₂ laser pulse,” *Appl. Phys. Lett.* **92**, 251501-1-251501-3, 2008.
- [9] P. K. Carroll and G. O’Sullivan, “Ground-state configurations of ionic species I through XVI for $Z = 57-74$ and the interpretation of $4d-4f$ emission resonances in laser-produced plasmas,” *Phys. Rev. A* **25**, 275-286, 1982.
- [10] G. O’Sullivan and P. K. Carroll, “ $4d-4f$ emission resonances in laser-produced plasmas,” *J. Opt. Soc. Am.* **71**, 227-230, 1981.
- [11] G. M. Zeng, H. Daido, T. Nishikawa, H. Takabe, S. Nakayama, H. Aritome, K. Murai, Y. Kato, M. Nakatsuka, and S. Nakai, “Soft x-ray spectra of highly ionized elements with atomic numbers ranging from 57 to 82 produced by compact lasers,” *J. Appl. Phys.* **75**, 1923-1930, 1994.
- [12] S. S. Churilov, R. R. Kildiyarova, A. N. Ryabtsev, and S. V. Sadovsky, “EUV spectra of Gd and Tb ions excited in laser-produced and vacuum spark plasmas,” *Phys. Scr.* **80**, 045303-1-045303-6, 2009.
- [13] T. Otsuka, D. Kilbane, J. White, T. Higashiguchi, N. Yugami, T. Yatagai, W. Jiang, A. Endo, P. Dunne, and G. O’Sullivan, “Rare-earth plasma extreme ultraviolet sources at 6.5–6.7 nm,” *Appl. Phys. Lett.* **97**, 111503-1-111503-3, 2010.
- [14] G. Mordovanakis, K.-C. Hou, Y.-C. Chang, M.-Y. Cheng, J. Nees, B. Hou, A. Maksimchuk, G. Mourou, A. Galvanauskas, and B. Lafontain, “Demonstration of fiber-laser-produced plasma source and application to efficient extreme UV light generation,” *Opt. Lett.* **31**, 2517-2519, 2006.
- [15] D. Colombant and G. F. Tonon, “X-ray emission in laser-produced plasmas,” *J. Appl. Phys.* **44**, pp. 3524-3537, 1973.
- [16] M. F. Gu, “Indirect X-Ray Line-Formation Processes in Iron L-Shell Ions,” *Astrophysical J.* **582**, 1241-1250, 2003.
- [17] T. Otsuka, D. Kilbane, T. Higashiguchi, N. Yugami, T. Yatagai, W. Jiang, A. Endo, P. Dunne, and G. O’Sullivan, “Systematic investigation of self-absorption and conversion efficiency of 6.7 nm extreme ultraviolet sources,” *Appl. Phys. Lett.* **97**, 231503-1-231503-3, 2010.

- [18] G. Tallents, E. Wagenaars, and G Pert, "Lithography at EUV Wavelengths," *Nature Photonics* **4**, 809-811, 2010.
- [19] J. White, P. Dunne, P. Hayden, F. O'Reilly, and G. O'Sullivan, "Optimizing 13.5 nm laser-produced tin plasma emission as a function of laser wavelength," *Appl. Phys. Lett.* **90**, 181502-1-181502-3, 2007.
- [20] T. Higashiguchi, K. Kawasaki, W. Sasaki, and S. Kubodera, "Enhancement of extreme ultraviolet emission from a lithium plasma by use of dual laser pulses," *Appl. Phys. Lett.* **88**, pp. 161502-1-161502-3, 2006.
- [21] T. Higashiguchi, N. Dojyo, M. Hamada, W. Sasaki, and S. Kubodera, "Low-debris, efficient laser-produced plasma extreme ultraviolet source by use of a regenerative liquid microjet target containing tin dioxide (SnO₂) nanoparticles," *Appl. Phys. Lett.* **88**, pp. 201503-1-201503-3, 2006.
- [22] A. Sasaki, K. Nishihara, M. Murakami, F. Koike, T. Kagawa, T. Nishikawa, K. Fujima, T. Kawamura, and H. Furukawa, "Effect of the satellite lines and opacity on the extreme ultraviolet emission from high-density Xe plasmas," *Appl. Phys. Lett.* **85**, 5857-5859, 2004.
- [23] S. Miyamoto, A. Shimoura, S. Amano, K. Fukugaki, H. Kinugasa, T. Inoue, and T. Mochizuki, "Laser wavelength and spot diameter dependence of extreme ultraviolet conversion efficiency in ω , 2ω , and 3ω Nd:YAG laser-produced plasmas," *Appl. Phys. Lett.* **86**, 261502-1-261502-3, 2005.
- [24] P. Hayden, A. Cummings, N. Murphy, G. O'Sullivan, P. Sheridan, J. White, and P. Dunne, "13.5 nm extreme ultraviolet emission from tin based laser produced plasma sources," *J. Appl. Phys.* **99**, 093302-1-093302-4, 2006.
- [25] T. Okuno, S. Fujioka, H. Nishimura, Y. Tao, K. Nagai, Q. Gu, N. Ueda, T. Ando, K. Nishihara, T. Norimatsu, N. Miyanaga, Y. Izawa, and K. Mima, "Low-density tin targets for efficient extreme ultraviolet light emission from laser-produced plasmas," *Appl. Phys. Lett.* **88**, 161501-1-161501-3, 2006.
- [26] D. Kilbane and G. O'Sullivan, "Ground-state configurations and unresolved transition arrays in extreme ultraviolet spectra of lanthanide ions" *Phys. Rev. A* **82**, 062504-1-062504-6, 2010.